doi:10.2533/chimia.2017.550 Chimia 71 (2017) 550–557

Renaissance of an Old Topic: From Borazines to BN-doped Nanographenes

María Mercedes Lorenzo-García and Davide Bonifazi*

Abstract: Graphene is one of the leading materials in today's science, but the lack of a band gap limits its application to replace semiconductors in optoelectronic devices. To overcome this limitation, the replacement of C=C bonds by isostructural and isoelectronic bonds is emerging as an effective strategy to open a band gap in monoatomic graphene layers. First prepared by Stock and Pohland in 1926, borazine is the isoelectronic and isostructural inorganic analogue of benzene, where the C=C bonds are replaced by B–N couples. The strong polarity of the BN bonds widens the molecular HOMO–LUMO gap, imparting strong UV-emission/absorption and electrical insulating properties. These properties make borazine a valuable molecular scaffold to be inserted as doping units in graphitic-based carbon materials to tailor a relevant band gap. It is with this objective that we became interested in the development of new synthetic organic methodologies to gain access to functionalized borazine derivatives. In particular, we have described the synthesis of borazine derivatives that, featuring aryl substituents at the B-centers bearing *ortho*-functionalities, are exceptionally stable against hydrolysis. Building on these structural motifs, we prepared hybrid BN-doped polyphenylene nanostructures featuring controlled doping patterns, both as dosage and orientation. Finally, exploiting the Friedel-Craft electrophilic aromatic substitution, we could develop the first rational synthesis of the first soluble hexa-peri-hexabenzoborazinocoronene and measured its optoelectronic properties, showing a widening of its gap compared to its full-carbon congener.

Keywords: 2D BN-doped networks · Band gap · BN-doped · Borazines · Graphene · Nanographene · Polyphenylenes

1. Introduction

1.1 *BN-doped Carbon Nanostructures*

Since the discovery from Geim and Novoselov in 2004,[1] in which graphene was experimentally confirmed for the first time, the field has known an unprecedented expansion within the scientific community. However, the lack of a band gap hampers graphene's possible applications as semiconducting material in optoelectronic devices.[2–4] To overcome this limitation, different strategies have been developed, including covalent and non-covalent functionalization approaches.[2,5–9] Above all, covalent doping, *i.e.* the substitution of C atoms with isostructural analogues, is becoming one of the most promising approaches.[10–12] In particular, the substitution of C=C bonds with isoelectronic and isostructural boron–nitrogen[10,12–14] couples is certainly the most efficient method to gain control of the molecular band gap (Fig. 1).[15–17] The strong polarity of the BN bond imparts a series of particular physical and structural properties, namely a widening of the HOMO-LUMO gap along with an increase of the HOMO energy level with respect to the all carbon analogues. For instance, Schwingenschlögl and co-workers showed that the BN-doping of monolayered, bilayered, trilayered and multilayered graphene triggered the appearance of a band gap.[18] In a BNC monolayer, the band gap can vary from 0.02 eV to 2.43 eV, depending on the doping percentage (from 12.5% to 75%).

Experimentally, the group of Wang recently published the preparation of BNC-nanosheets by pyrolysis of glucose, boron oxide and urea at 1250 ºC.[19] These sheets were successfully used as photocatalysts for water splitting under visible irradiation. The *h*-BNC band gaps (2–3 eV) were estimated to straddle the water redox potentials, making H_2 generation as well as the O_2 evolution possible (when coupled to Ni-Co layered co-catalyst). In a parallel experiment, they also used the *h*-BNC to photochemically reduce CO_2 into CO. Compared to other photocatalysts like TiO_2 or *g*-C_3N_4, BNC hybrids exhibit better catalytic performance and photostability. Following the same synthetic approach, they have also prepared porous BNC nanosheets for the oxidative dehydrogenation of alkanes such as ethylbenzene.[20] This work represents an important advance as this catalyst presents an oxidation resistance that avoids the deactivation of the material. Along similar lines, Ajayan and co-workers described in 2010 the preparation of hybrid *h*-BNC monolayers, obtained by chemical vapor deposition (CVD) using copper as substrate and a mixture of CH_4 and ammonia borane as carbon and BN sources, respectively.[21] By controlling the experimental parameters (temperature, time and

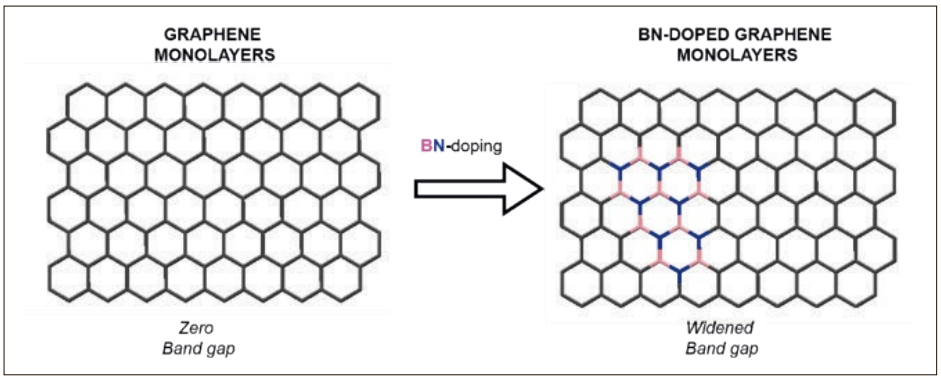

Fig. 1. Schematic representation of band gap tuning by substitution of carbon atoms with boron and nitrogen atoms in a graphitic monolayer.

*Correspondence: Prof. D. Bonifazi
School of Chemistry, Cardiff University
Park Place, Main Building
Cardiff, CF10 3AT, UK
E-mail: bonifazid@cardiff.ac.uk

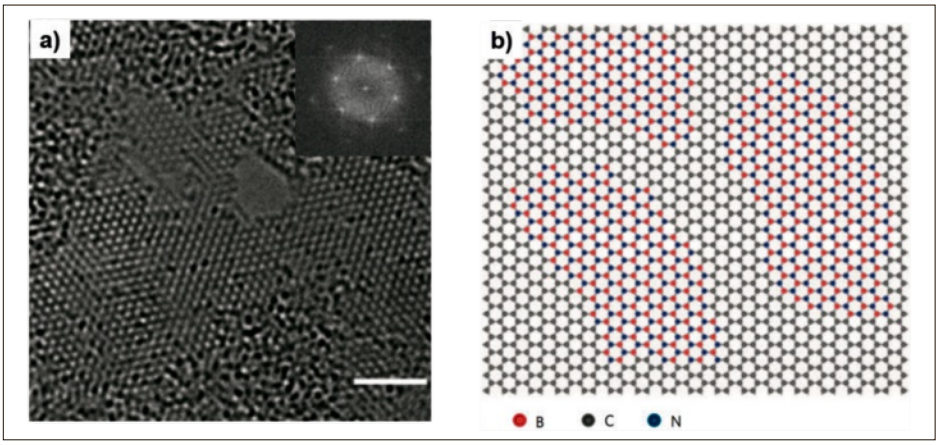

Fig. 2. a) An HRTEM image of a single-layer region of the *h*-BNC film. Scale bars: 2 nm. Inset: FFT pattern of the single-layer region, b) Atomic model of the *h*-BNC film displaying hybridized *h*-BN and graphene domains.[21] Reprinted with permission from ref. [21]. Copyright (2010) Nature Publishing Group.

feedstock ratio), they were able to control the BN-doping from 10% to ~100%. All prepared structures showed segregated carbon and BN domains (Fig. 2).

In 2013, Jiong *et al.* performed a study of a two-dimensional BNC alloy on ruthenium surfaces using scanning tunneling microscopy (STM).[22] Upon treatment of a Ru (0001)-grown graphene monolayer with vaporized borazine at 900 K, carbon etching and replacement with boron and nitrogen atoms (obtained from the decomposition of the borazine) formed a brick-and-mortar pattern following the moiré pattern of graphene (Fig. 3, a-b and c-f). The moiré pattern of graphene on Ru(0001), which comes from the differences in crystal lattices of the graphene and the ruthenium surfaces, leads to periodic domains where C atoms are displaced vertically, close to ruthenium atoms and domains in which C atoms are further away from the metal surface, forming a graphene landscape with humps and valleys. In the valleys, the vicinity of the C atoms to the ruthenium surface can catalyze the reduction of the graphene layer by the borazine thermal decomposition products (B, N, and H reactive species), etching away the C atoms, and incorporating B and N atoms into the graphene structure (Fig. 3b).

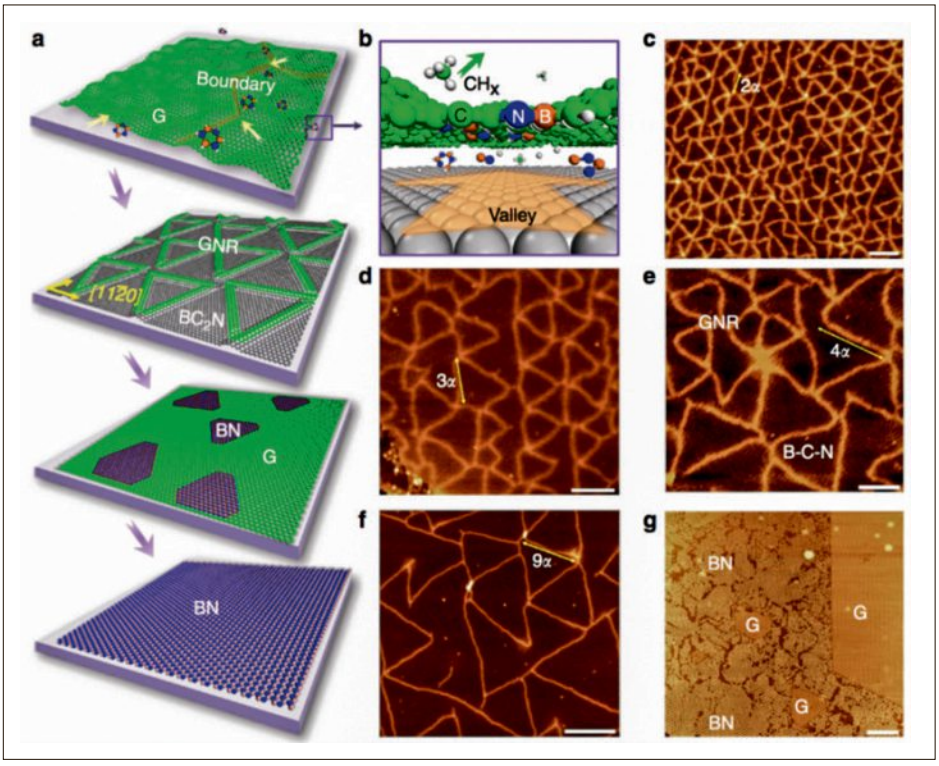

Fig. 3. Synthesis of mixed BNC domains enclosed by GNRs. a) Image of the substitutional doping of G/Ru(0001) by borazine, leading to the formation of brick-and-mortar pattern, domain-wise G-BN mosaic film and a complete replacement of carbon into the BN framework; b) Schematic representation showing the sub-surface diffusion and catalytic decomposition of borazine to generate B and N species which replace lattice carbon in graphene; c) Phase segregated GNRs modulated by the moiré pattern; d–f) STM images show the evolution of mixed BNC domains (dotted dark) and demixed GNR phases (bright lines) upon the stepwise dosing of borazine at 900 K; g) The formation of domain-wise G-BN composite by a complete phase segregation in BNC at 900 K. Scale bars in (c–g) are 6, 10, 6, 25 and 40 nm, respectively. Reprinted with permission from ref. [22]. Copyright (2013) Nature Publishing Group.

By increasing the BN dosage, mixed BNC domains were formed with an average composition equivalent to *h*-BNC, encapsulated by graphene nanoribbon threads (Fig. 3, c-f). By careful control of temperature and borazine dosage, the authors were able to grow mixed *h*-BNC layers with a measured band gap of 2 eV, very close to that theoretically calculated for *h*-BNC (1.6 eV). Irradiation at 532 nm of the hybrid layer showed strong photoluminescence centered at 590 nm (2.1 eV), in contrast to graphene or *h*-BN layers which are non-emissive. Recently, Enders and co-workers presented an ingenious synthesis of BNC monolayers, using bis-BN cyclohexane as precursor for an ordered growth on Ir(111) substrates, at high temperatures under ultrahigh vacuum.[23] To our knowledge, this work describes the best example of full ordered BN-doped graphene sheets. At the molecular level, several synthetic methods allowed the preparation of a large number of BN-doped aromatic derivatives,[24–26] from azaborines[27] to extended polycyclic aromatic hydrocarbons. In particular, BN-doped naphthalenes, anthracenes, or phenanthrenes could be prepared by diverse synthetic strategies, including $AlCl_3$-promoted electrophilic borylation method of arylamines,[28] cyclization–dehydrogenation procedures,[29] or *via* chelation of bis-borabiphenyl precursors with pyridazine derivatives.[30] For example, Nakamura and co-workers described in 2011 a renewed strategy for the synthesis of BN-doped frameworks,[31] *via* tandem intramolecular electrophilic arene borylation. As a proof of concept, Zhang[25] and Pei[26] simultaneously developed the synthesis of a BN-embedded coronene-type molecule.

1.2 *Borazines as Doping Units*

In order to control the BN-doping of graphitic molecules, the introduction of doping units possessing similar structural properties to those of benzene appears as the natural direction. Among the BN-based structures, borazine, also known as 'inorganic benzene', represents an appealing building block to design hybrid molecular graphenes due to its structural (planar hexagonal structure with a bond length of

1.436 Å for borazine, between B–N single bond at 1.51 Å and B-N double bond at 1.31 Å) and physical (both are liquids at rt) similarities to benzene. Being only weakly aromatic, borazines tend to undergo hydrolysis to form boric acid and ammonia in the presence of humidity. Therefore, if one wants to prepare derivatives that are stable under moisture conditions, steric protection is needed at the boron centers. Also, compared to benzene and its polycyclic derivatives, borazines display wide HOMO–LUMO gaps due to the strong polar character of the BN bonds.

By now, it is apparent that borazines can represent versatile doping units to be inserted in full-carbon nanographene. Among the different approaches, bottom-up covalent synthesis is certainly the most reliable approach toward controlled insertion of the BN ring as it should avoid segregation phenomena. This method allows the introduction of the doping borazine ring units in different ratios, orientations, and positions (Fig. 4) following these parameters: the doping dosage (r); the doping orientation (o), and the doping vector (d_i). Taken all together, the three descriptors r, d_i and o allow the precise depiction of the borazine-doping pattern of any hybrid hexagonal polycyclic aromatic structure. Our group has recently contributed to the field, with i) the extension of BN-doped polycyclic aromatic hydrocarbons (PAHs) into dendritic structures and ii) the planarization of BN-doped polyphenylenes into the first nanographene system.

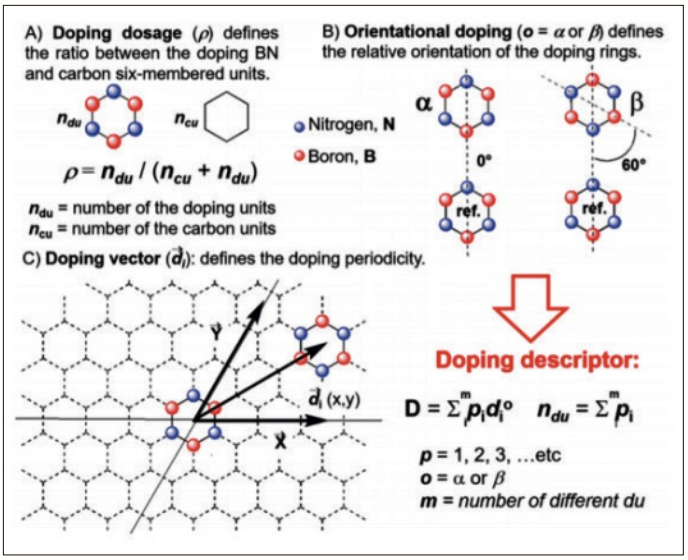

Fig. 4. Descriptors for the BN-doping of polyphenylenes and BN-doped PAHs. Reprinted with permission from ref. [33]. Copyright (2017) American Chemical Society.

2. Borazine Synthesis

A borazine cycle can be prepared following two approaches (Fig. 5): either *via* a [1+1'+1+1'+1+1'] hexamerization route from a mixture of the relevant borane (*i.e.* hydro or halide) and amino precursors, or through a [2+2+2] trimerization approach using a pre-formed imino or aminoborane derivative.[11] Depending on the borane nature, different reactions have been used: condensation reactions with BX_3 (X = Br or Cl) and thermal or metal-catalyzed dehydrogenation with boron hydrides.[32,34–37]

In particular, following the BCl_3-based methodology, for which a *B,B',B"*-trichloro borazine intermediate is formed in the presence of an amine in anhydrous toluene at high temperatures, alkyl or aryl substituents at the boron centers can be subsequently added through substitution reactions upon addition of the relevant organometallic (RLi or RMgBr) species (Fig. 6).[38,39] Depending on the stoichiometry and the addition sequence of the organometallic species, the method is versatile and allows the formation of borazines featuring different substitution patterns, like $A_3B_3N_3E_3$, $A_2CB_3N_3E_3$ and $ACDB_3N_3E_3$ (where A, C, D and E are the boron and nitrogen substituents, respectively). In a recent example, Yamaguchi and co-workers reported the preparation of anthryl-bearing borazine **7**, following the BCl_3/RLi two-step approach (Fig. 6).[40] In their molecule, the anthryl hydrogen atoms sit atop the electrophilic boron centers from nucleophile additions, thus shielding them from nucleophilic addition and increasing the inertness of the BN cycle toward hydrolysis. Following this synthetic approach, we have prepared borazine derivative **2** (Fig. 6) that, when subjected to hydrolysis in water-containing mixtures, exhibited extraordinary stability. This suggested that the *ortho*-methyl substituents exert a steric hindrance chemically shielding the *B* atom centers. Fluorescence measurements in solution showed that borazine **2** is a blue emitter, displaying quantum yields (F_{em}) between 6.6% and 7.7%. Building on this approach, we prepared a large variety of different borazines, all featuring an extraordinary chemical stability toward hydrolysis (Fig. 6).

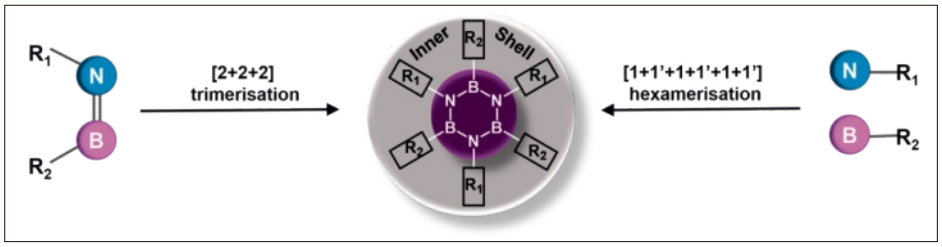

Fig. 5. Synthetic strategies toward the synthesis of the borazine core, with $R_1 = R_2$ or $R_1 \neq R_2$ being an aryl, alkyl or hydrogen substituent.[32,39]

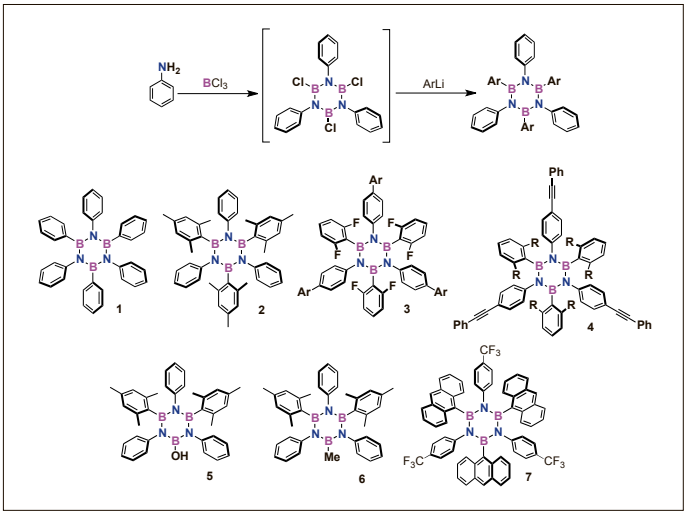

Fig. 6. Synthetic one-pot procedure for preparing borazines: condensation and organometallic addition steps.[40–44]

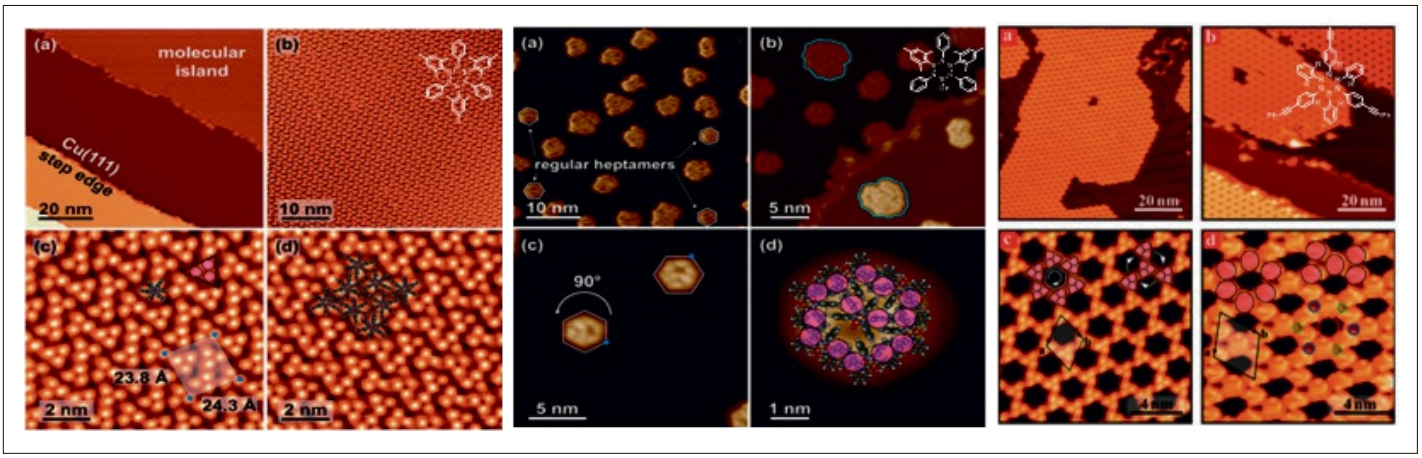

Fig. 7. LEFT: STM images for borazine **2** on Cu(111), deposited at 300 K, recorded at 77 K. a) Large area of the Cu(111) surface; b)–c) Expanded views of the molecular islands; the three circles in the triangle in c) correspond to the three Mes moieties; the shaded rectangle corresponds to the experimental unit cell. d) Calculated structure superimposed on the imaged monolayer. CENTER: STM images of borazine **5** on Cu(111). a) Isolated molecular clusters, highlighting the regular heptamers. b) Expanded view of a Cu(111) step edge, revealing two enantiomers of an irregular cluster. c) Expanded view of two 90°-rotated regular heptamers. d) Calculated molecular model superimposed onto the heptamer. RIGHT: STM images of borazine **4** deposited at r.t. on Au(111) and Cu(111). The images were acquired at 77 K. Expanded views (a-b) of the extended 2D molecular islands. Higher resolution images (c-d) of the porous networks.[42,44] Reprinted with permission from refs [42,44]. Copyright (2013 and 2014) Wiley.

In collaboration with the group of Prof. Franco Cacialli (UCL London), we used molecule **2** as UV-emitter in a light-emitting electrochemical cell (LEC).[41] Weak UV-emission was observed at high voltages (~15 V). Similar results were obtained for the corresponding LEDs, giving promising EL quantum efficiency values of ~10^{-4}% that, although rather weak, are the first of its kind. Beside the molecular and bulk material properties, the understanding of self-assembly behavior of borazines in molecular layers at surfaces is also important if one wants to fully appreciate the structural properties of the active interfaces exposed to an electrode.[45,46] In a collaborative venture with the groups led by Alessandro De Vita (King's College London) and Giovanni Costantini (University of Warwick), we have described the non-covalent bottom-up engineering of borazine-based architectures on metal surfaces.[42] By means of low-temperature (LT) scanning tunneling microscopy (STM) measurements, we have observed different networks depending on the aryl substituents. In particular, we have shown that borazines **2** and **5** undergo different molecular organization on Cu(111) surfaces. While molecule **2** self-organizes into full monolayers held together by van der Waals (vdW) interactions, borazine **5** bearing an OH function undergoes exclusive 'magic' clustering (Fig. 7). In a subsequent work, we have investigated the effect of the peripheral substituents (Fig. 7). Notably, when peripheral phenylethynyl substituents are present, molecule **4** interacts with the metal substrate, driving the formation of porous networks on Au(111) or Cu(111) surfaces.[44]

3. Branched Multiborazine Nanostructures

Dendritic polyphenylenes have played a pivotal role as chemical precursors for the bottom-up synthesis[3,47] of graphitic nanostructures. Hybrid polyphenylenes scaffoldings exposing borazine rings placed in selected positions could represent an unprecedented class of p-extended molecular BNC hybrid nanostructures, that could be used as precursors to prepare BN-doped nanographenes. Building on the sterically-protected borazine scaffold exposing aryl groups at the boron sites bearing *ortho*-methyl groups, we recently described the first divergent synthesis of borazino-doped polyphenylenes in which one or more aryl units are replaced by borazine rings. Exploiting the decarbonylative [4+2] Diels-Alder cycloaddition reaction between ethynyl and tetraphenylcyclopentadienone derivatives, we could prepare three- and hexa-branched hybrid polyphenylenes that feature controlled orientation and dosage of the doping B_3N_3-rings. These were achievable targets thanks to the possibility of functionalizing the borazine core with orthogonal reactive groups on the aryl substituents at the N and B atoms. The strategy included the preparation of two molecular modules: a core (bearing ethynyl moieties) and a branching (bearing the cyclopentadienone) module. Depending on the substitution pattern at the borazine core, the covalent combination of the modules yielded one exclusive dendritic structure for each particular doping pattern (Figs. 8 and 9).

Focusing on the emissive properties, we have figured out why, upon increasing the doping dosage, the strong luminescent signal is progressively reduced (F_{em} = 76% – 7%, Fig. 10). As it clearly appears from

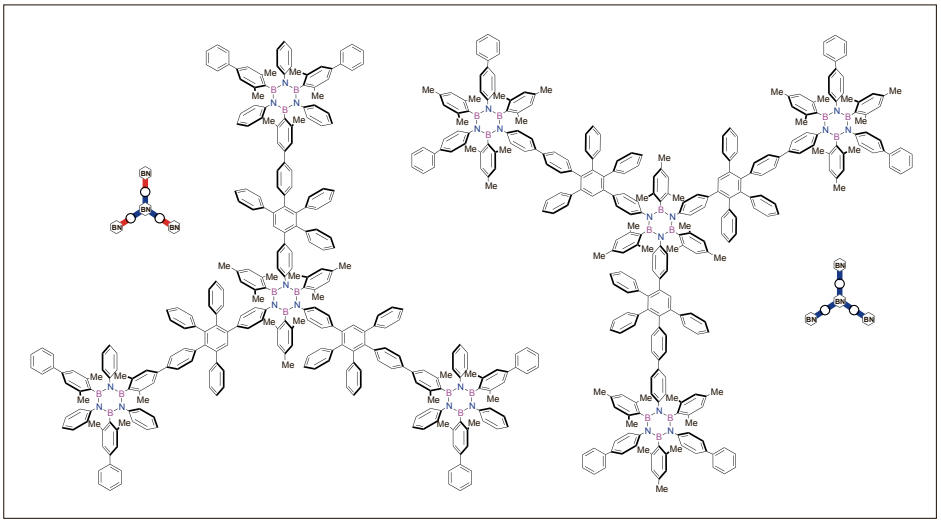

Fig. 8. Examples of structures of tribranched borazino-doped polyphenylenes.

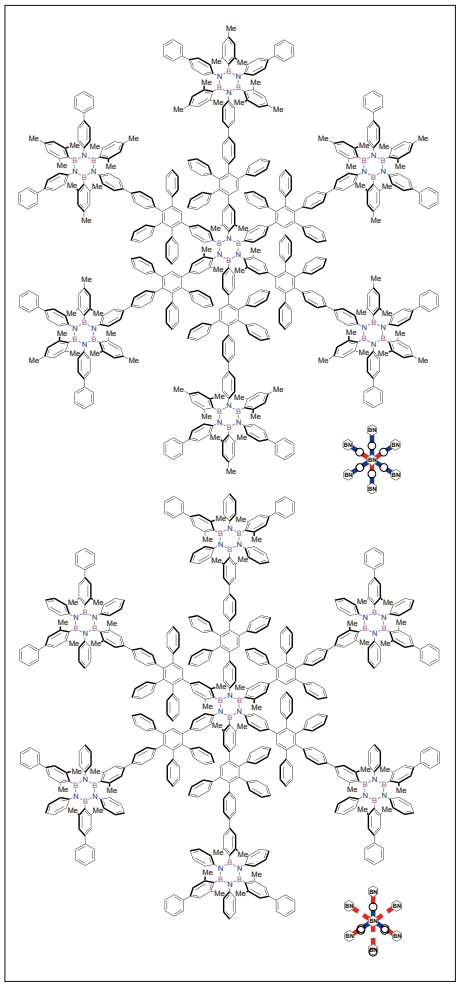

Fig. 9. Examples of structures of hexabranched borazino-doped polyphenylenes.

the experimentally calculated rate constants values, by increasing the BN dosage, the non-radiative deactivation of the singlet-excited states is accelerated. This suggests that the presence of the borazino rings engages additional deactivation pathways possibly involving excited states with an increasing charge separation character. This is likely to be limited in the full-carbon analogues. Notably, a strong effect of the orientational doping on the fluorescence quantum yields was observed for those hybrids featuring low doping BN dosages. Although this is the first rational bottom-up approach toward the preparation of a molecular BNC with a controlled doping pattern, the presence of the methyl substituents at the *ortho* positions of the *B*-aryl moieties handicaps any possible planarization attempts. It is now apparent that, although necessary for the chemical stability of the borazine, *ortho*-groups that can be activated to give C–C bonds are necessary if one wants to achieve the synthesis of BN-doped nanographenes.

4. Toward Borazino-doped Nanographenes

Earlier synthetic reports on the preparation of extended BN-doped graphenes by Bettinger and co-workers described the synthesis of derivative **11** (Fig. 11), in which three 9,10-BN-phenanthrenes are linked through a borazine core.[24]

In a first route, intermediate **9** was prepared by MW-assisted reaction of 2-aminobiphenyl with BCl_3 in the presence of $AlCl_3$.[48] Either through direct transformation or *via* the triflate derivative (**10**), base-induced elimination reaction gave borazine **11** through cycloaddition-type reactions involving a BN-aryne intermediate. Alternatively, cyclotrimer **11** could be obtained by thermolysis of borazine **12**, the latter being prepared from 2-aminophenyl and $Et_3N{\cdot}BH_3$ at 205 °C. Through pyrolysis at 550 °C, the first un-substituted hexa-*peri*-hexabenzoborazinocoronene (**8**) could be identify by mass-spectrometry (as well as derivative **12**). However, the poor solubility of this molecule did not allow an 'in-depth' study of its optoelectronic properties. Our contribution to the field has been recognized with the first rational synthesis of a substituted hexa-*peri*-hexabenzoborazinocoronene (HBBNC) that, being soluble in common organic solvents, allowed a direct comparison of optoelectronic properties with those of its full-carbon congener. At the synthetic level, the planarization of aryl moieties into polycyclic aromatic hydrocarbons are usually obtained through Scholl-type oxidative ring-closure reactions.[3,49] However, the vulnerability of the borazine ring under oxidative conditions[11] precludes the use of any oxidizing routes and thus guided us towards Friedel-Craft-type substitution reactions as planarization strategy. Embracing this synthetic route, we prepared a borazine precursor **3** bearing F at *ortho*-positions of the *B*-aryl substituents and peripheral xylyl moieties as solubilizing groups. Taking advantage of the Friedel-Crafts ring-closure reaction of fluoroarenes, developed by Siegel and co-workers,[50] planarization of the hexa-fluoro borazine yielded desired HBBNC **14** in the presence of $[iPr_3Si{\cdots}CB_{11}H_6Cl_6]$ and Me_2SiMe_2 at 110 ºC in PhCl (Fig. 12).[43] This work marks an important milestone in the synthesis of controlled BN-doped nanographene molecules, even though this synthetic route is limited due to the low yield of the reaction (5% in total, 61% per C–C bond formation).

X-ray analysis showed the nearly flat shape of the BN-doped molecule (similar to the all-carbon analogue).

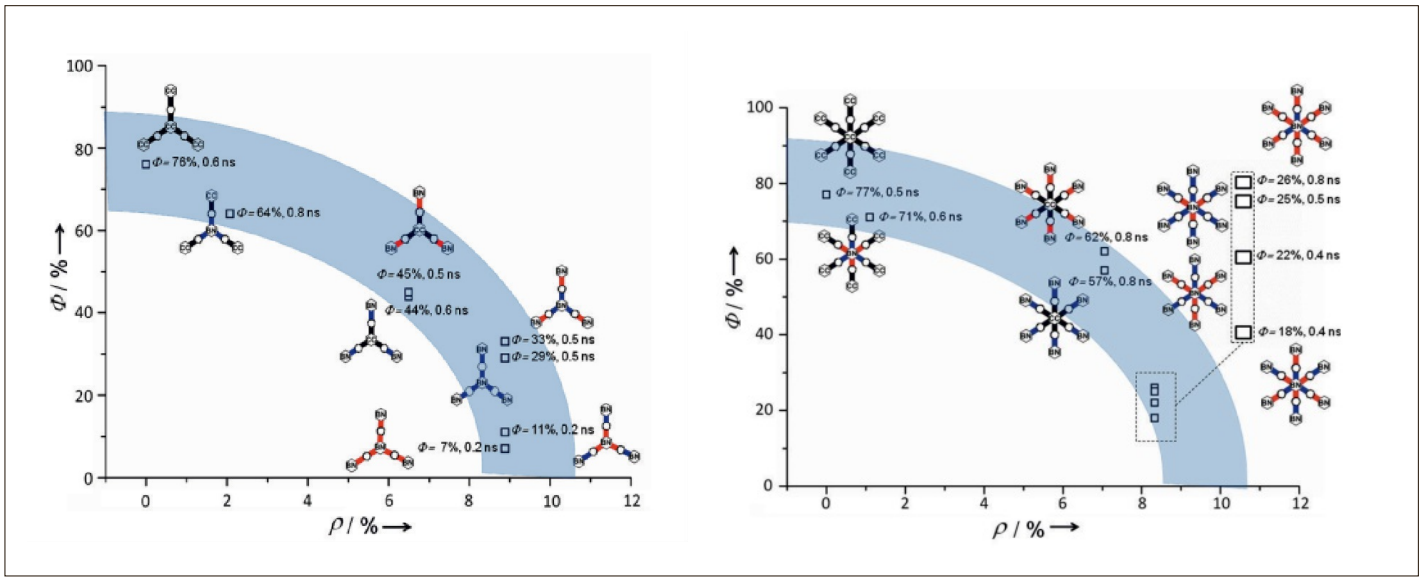

Fig. 10. Emission quantum yield as a function of the dosage and orientational doping for tri- and hexabranched borazino-doped polyphenylenes. Reprinted with permission from ref. [33]. Copyright (2017) American Chemical Society.

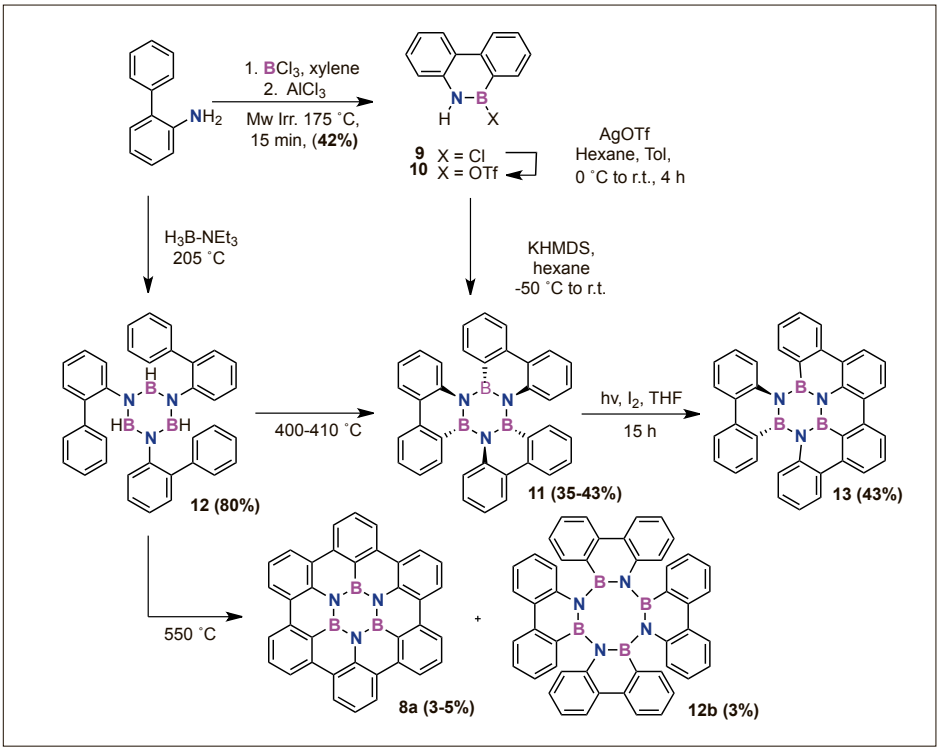

Fig. 11. Synthesis of the first borazino-doped hexabenzocoronene by Bettinger *et al*.[24]

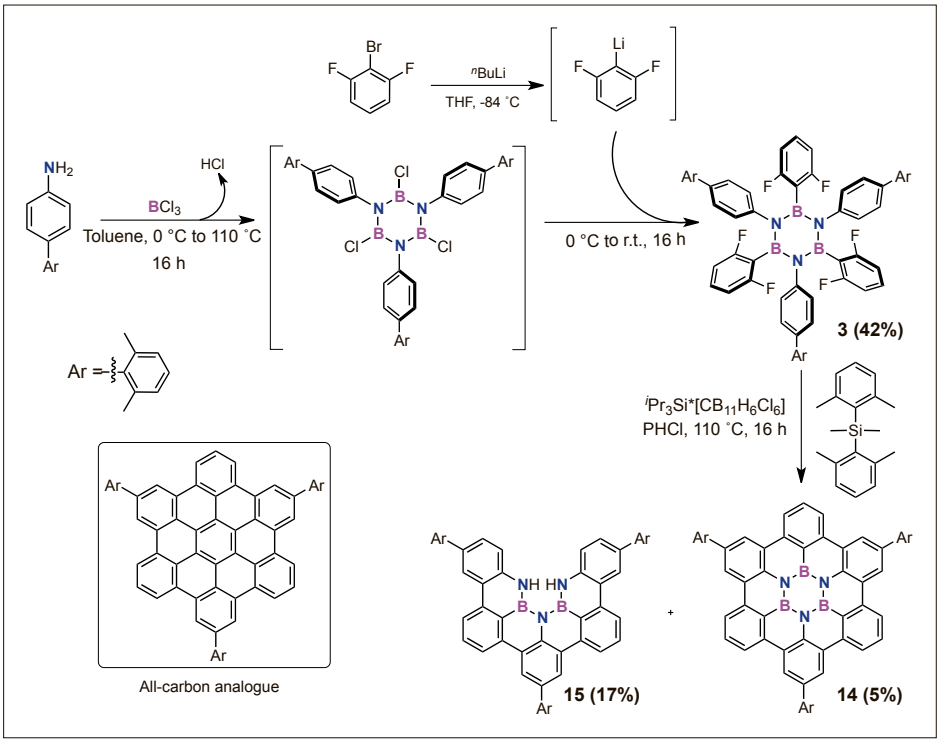

Fig. 12. Friedel-Craft synthetic route allowing the preparation of the hexa-*peri*-hexabenzoborazinocoronene **14** (HBBNC); inset: molecular structure of HBC.

Furthermore, the photophysical studies of both the BN-doped derivative and the all-carbon one confirmed the expected widening of the band gap in the BN-doped molecule, as well as the blue-shift with respect to the all-carbon analogue (Fig. 13). The all-carbon analogue (HBC) was also prepared in order to compare the intrinsic properties of both molecules.

Following these seminal investigations about the self-assembly behavior of borazine derivatives on metal surfaces, Sánchez-Sánchez *et al*. reported recently the surface-assisted polymerization and cyclodehydrogenation reaction of two distinct borazine derivatives on Ag(111) surfaces: tri-bromophenyl borazine **16** and 2,12,22-tribromo-tri(*o*,*o*'-biphenyl-yl)borazine (not shown here). By means of this stepwise thermal methodology, interlinked BN-HBC networks could be prepared on a Ag(111) surface under ultra-high vacuum (UHV) conditions.[51] In particular, thermal deposition of **16** on Ag(111) led to the formation of non-covalent flower-like assemblies at 425 K (Fig. 14a). When the temperature is increased to 475 K, phenyl-phenyl type cross-coupling reactions catalyzed by Ag atoms occurred at the C–Br functionalities (Fig. 14b), forming covalently assembled networks. Complete cyclodehydrogenation of partially planarized molecule **16** could be achieved at 575 K (Fig. 14c), ultimately leading to the formation of the covalently-linked borazino coronone network. Together with the first self-assembly studies on surfaces, this represents the first step toward the implementation of the BN-doped hybrid carbon materials and the assessment of their real electronic properties and potentials applications in molecular devices.

5. Conclusions

The rise of graphene as a wonderful material has inspired a lot of research activities in physical science. In particular, the synthetic attempts to introduce an electronic gap triggering the appearance of semiconductor behavior is one of the main focuses in today's organic materials science. Among the different strategies, the replacement of the C=C double bonds with isostructural YX atom couples that, possessing different periodic properties, would modulate the HOMO–LUMO properties is certainly one of the most interesting approaches. In this respect, we believe that borazine would represent an ideal structural candidate to be merged with its carbon congener and prepare hybrid BNC structures featuring programmed optoelectronic properties. However, if one wants to explore the full potential of these structures, the chemistry of borazine needs to be fully developed and understood at the same level as that of benzene. In the last years, we have undertaken a research program in the field aimed at the development of organic chemistry methods that would allow a controlled functionalization of the borazine cycle and that of the aryl substituents on both N and B centers. In particular, we discovered that the presence of functional groups at the *ortho* position of the *B*-aryl substituents sterically shields the boron atoms, making the ring inert toward hydrolysis (even in boiling water) and thus

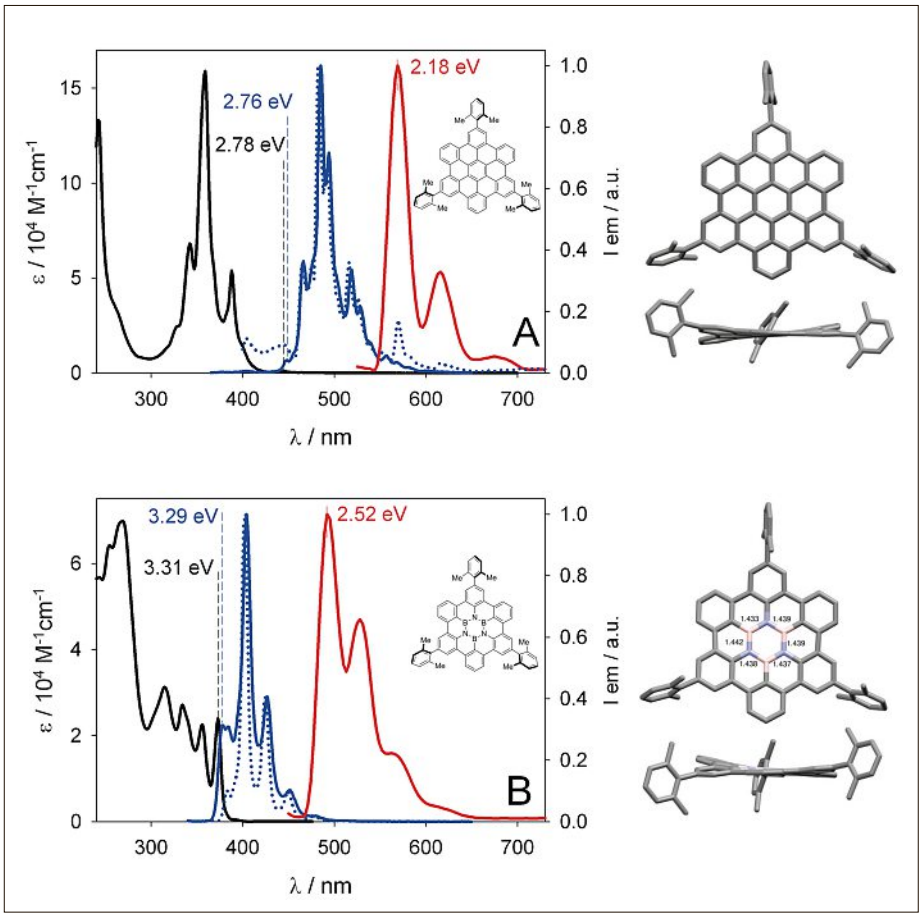

Fig. 13. Absorption (black), normalized fluorescence (blue) spectra (air equilibrated CH_2Cl_2 at r.t.) and horizontal (top) and side (bottom) view of the X-ray crystal structures of HBC (A) and HBBNC (B); fluorescence (blue dotted) and phosphorescence (red) spectra at 77 K in a CH_2Cl_2:CH_3OH (1:1 v/v) rigid matrix. Reprinted with permission from ref. [43]. Copyright (2017) Wiley..

chemically stable. This allowed us to extend the chemical space of this molecule, giving access to a large variety of borazine derivatives. In particular, through the exploitation of Sonogashira-type cross-coupling and [4+2] Diels-Alder cycloaddition reactions, we could engineer unprecedented borazino-doped polyphenylene derivatives featuring precise doping patterns. Depending on the relative orientation of the doping units and the doping dosage, we observed different emissive properties, with the latter being most affected at high doping dosages. In a parallel endeavor, we could develop the first rational synthesis of a benzocorone scaffold featuring a borazino core through six intramolecular Friedel-Crafts-type cyclization reactions. Extensive electrochemical and photophysical characterization of the BN-doped derivative showed a wider band gap with enhanced, blueshifted emission when compared to its full-carbon congener. Nevertheless, the low yield for the full cyclization calls for the development of more efficient synthetic strategies that, being compatible with the BN ring, will allow the planarization of extended BN-doped macromolecular systems. Together with the objective of expanding the organic chemical space of borazine, the search of non-oxidative planarization strategies will be the synthetic challenge of our future endeavors in the molecular BNC field.

Received: July 26, 2017

[1] K. S. Novoselov, A. K. Geim, S. V. Morozov, D. Jiang, Y. Zhang, S. V. Dubonos, I. V. Grigorieva, A. A. Firsov, *Science* **2004**, *306*, 666.
[2] F. Schwierz, *Nat. Nanotechnol.* **2010**, *5*, 487.
[3] A. Narita, X.-Y. Wang, X. Feng, K. Müllen, *Chem. Soc. Rev.* **2015**, *44*, 6616.
[4] J. Wu, W. Pisula, K. Müllen, *Chem. Rev.* **2007**, *107*, 718.
[5] T. Ohta, A. Bostwick, T. Seyller, K. Horn, E. Rotenberg, *Science* **2006**, *313*, 951.
[6] Y. Zhang, T.-T. Tang, C. Girit, Z. Hao, M. C. Martin, A. Zettl, M. F. Crommie, Y. R. Shen, F. Wang, *Nature* **2009**, *459*, 820.
[7] C. R. Dean, A. F. Young, I. Meric, C. Lee, L. Wang, S. Sorgenfrei, K. Watanabe, T. Taniguchi, P. Kim, K. L. Shepard, J. Hone, *Nat. Nanotechnol.* **2010**, *5*, 722.
[8] G. Lu, K. Yu, Z. Wen, J. Chen, *Nanoscale* **2013**, *5*, 1353.
[9] L. Chen, Y. Hernandez, X. Feng, K. Müllen, *Angew. Chem. Int. Ed.* **2012**, *51*, 7640.
[10] H. Helten, *Chem. - A Eur. J.* **2016**, *22*, 12972.
[11] D. Bonifazi, F. Fasano, M. M. Lorenzo-Garcia, D. Marinelli, H. Oubaha, J. Tasseroul, *Chem. Commun.* **2015**, *51*, 15222.
[12] X. Y. Wang, J. Y. Wang, J. Pei, *Chem. Eur. J.* **2015**, *21*, 3528.
[13] Z. Liu, T. B. Marder, *Angew. Chem. Int. Ed.* **2008**, *47*, 242.
[14] P. G. Campbell, A. J. V. Marwitz, S.-Y. Liu, *Angew. Chem. Int. Ed.* **2012**, *51*, 6074.
[15] W. Xie, T. Yanase, T. Nagahama, T. Shimada, *Carbon Res.* **2016**, *2*, 2.
[16] N. Otero, K. E. El-Kelany, C. Pouchan, M. Ré Rat, P. Karamanis, *Phys. Chem. Chem. Phys.* **2016**, *18*, 25315.
[17] N. Otero, P. Karamanis, K. E. El-Kelany, M. Rérat, L. Maschio, B. Civalleri, B. Kirtman, *J. Phys. Chem.* **2017**, *121*, 709.
[18] T. P. Kaloni, R. P. Joshi, N. P. Adhikari, U. Schwingenschlögl, *Appl. Phys. Lett.* **2014**, *104*, 073116.
[19] C. Huang, C. Chen, M. Zhang, L. Lin, X. Ye, S. Lin, M. Antonietti, X. Wang, *Nat. Commun.* **2015**, *6*, 7698.
[20] F. Guo, P. Yang, Z. Pan, X.-N. Cao, Z. Xie, X. Wang, *Angew. Chem. Int. Ed.* **2017**, *56*, DOI 10.1002/ange.201703789.
[21] L. Ci, L. Song, C. Jin, D. Jariwala, D. Wu, Y. Li, A. Srivastava, Z. F. Wang, K. Storr, L. Balicas, F. Liu, P. M. Ajayan, *Nat. Mater.* **2010**, *9*, 430.
[22] L. Jiong, Z. Kai, L. Xin Feng, H. Zhang, T. C. Sum, A. H. Castro Neto, K. P. Loh, *Nat. Commun.* **2013**, *4*, 2681.
[23] S. Beniwal, J. Hooper, D. P. Miller, P. S. Costa, G. Chen, S.-Y. Liu, P. A. Dowben, E. Charles, H. Sykes, E. Zurek, A. Enders, *ACS Nano* **2017**, *11*, 2486.
[24] M. Krieg, F. Reicherter, P. Haiss, M. Ströbele, K. Eichele, M. J. Treanor, R. Schaub, H. F. Bettinger, *Angew. Chem. Int. Ed.* **2015**, *54*, 8284.
[25] G. Li, W.-W. Xiong, P.-Y. Gu, J. Cao, J. Zhu, R. Ganguly, Y. Li, A. C. Grimsdale, Q. Zhang, *Org. Lett.* **2015**, *17*, 560.
[26] X.-Y. Wang, F.-D. Zhuang, R.-B. Wang, X.-C. Wang, X.-Y. Cao, J.-Y. Wang, J. Pei, *J. Am. Chem. Soc.* **2014**, *136*, 3764.
[27] M. J. S. Dewar, *J. Am. Chem. Soc.* **1962**, *84*, 3782.
[28] S. S. Chissick, M. J. S. Dewar, P. M. Maitlis, *Tetrahedron Lett.* **1960**, *1*, 8.
[29] K. M. Davies, M. J. S. Dewar, P. Rona, *J. Am. Chem. Soc.* **1967**, *89*, 6294.
[30] D. J. H. Emslie, W. E. P. Piers, M. Parvez, *Angew. Chem. Int. Ed.* **2003**, *42*, 1251.
[31] T. Hatakeyama, S. Hashimoto, S. Seki, M. Nakamura, *J. Am. Chem. Soc.* **2011**, *133*, 18614.
[32] A. Stock, E. Pohland, *Ber. Dtsch. Chem. Ges. B Ser.* **1926**, *59*, 2210.
[33] D. Marinelli, F. Fasano, B. Najjari, N. Demitri, D. Bonifazi, *J. Am. Chem. Soc.* **2017**, *139*, 5503.
[34] H. I. Schlesinger, D. M. Ritter, A. B. Burg, *J. Am. Chem. Soc.* **1938**, *60*, 1296.
[35] G. W. Schaeffer, R. Schaeffer, H. I. Schlesinger, *J. Am. Chem. Soc.* **1951**, *73*, 1612.
[36] E. Framery, M. Vaultier, *Heteroat. Chem.* **2000**, *11*, 218.
[37] T. Wideman, L. Sneddon, *Inorg. Chem.* **1995**, *34*, 1002.
[38] A. W. Laubencayer, C. A. Brown, *J. Am. Chem. Soc.* **1955**, *77*, 3699.
[39] J. H. Smalley, S. F. Stafiej, *J. Am. Chem. Soc.* **1959**, *81*, 582.
[40] A. Wakamiya, T. Ide, S. Yamaguchi, *J. Am. Chem. Soc.* **2005**, *127*, 14859.
[41] S. Kervyn, O. Fenwick, F. Di Stasio, Y. S. Shin, J. Wouters, G. Accorsi, S. Osella, D. Beljonne, F. Cacialli, D. Bonifazi, *Chem. Eur. J.* **2013**, *19*, 7771.

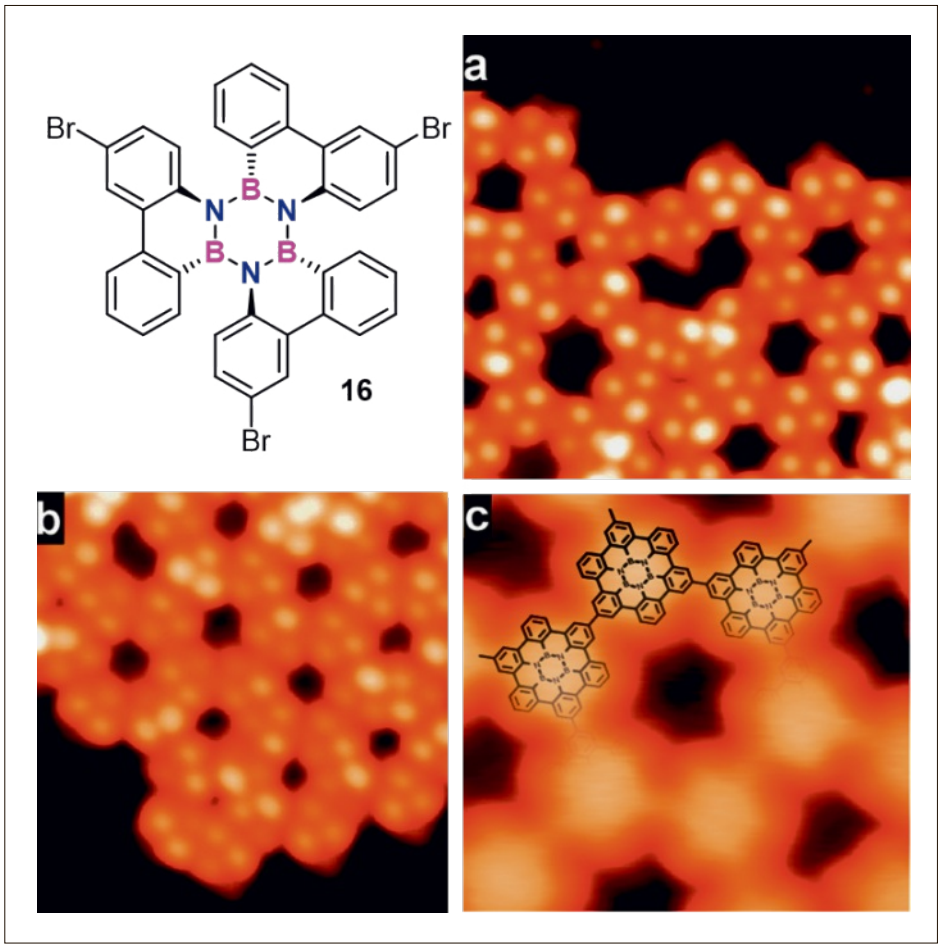

Fig. 14. Molecular structure of **16**. a) STM images after deposition. b) Covalent network after polymerization at 475 K. c) High resolution STM of the planar network after cyclodehydrogenation at 575 K. Reprinted with permission from ref. [51]. Copyright (2015) American Chemical Society.

[42] S. Kervyn, N. Kalashnyk, M. Riello, B. Moreton, J. Tasseroul, J. Wouters, T. S. Jones, A. De Vita, G. Costantini, D. Bonifazi, *Angew. Chem. Int. Ed.* **2013**, *52*, 7410.
[43] J. Dosso, J. Tasseroul, F. Fasano, D. Marinelli, N. Biot, A. Fermi, D. Bonifazi, *Angew. Chem. Int. Ed.* **2017**, *56*, 4483.
[44] N. Kalashnyk, P. Ganesh Nagaswaran, S. Kervyn, M. Riello, B. Moreton, T. S. Jones, A. De Vita, D. Bonifazi, G. Costantini, *Chem. Eur. J.* **2014**, *20*, 11856.
[45] S. R. Forrest, *Nature* **2004**, *428*, 911.
[46] A. R. Murphy, J. M. J. Fréchet, *Chem. Rev.* **2007**, *104*, 1066.
[47] L. Dössel, L. Gherghel, X. Feng, K. Müllen, *Angew. Chem. Int. Ed.* **2011**, *50*, 2540.
[48] M. J. D. Bosdet, C. A. Jaska, W. E. Piers, T. S. Sorensen, M. Parvez, *Org. Lett.* **2007**, *9*, 1395.
[49] M. D. Watson, A. Fechtenkötter, K. Müllen, *Chem. Rev.* **2001**, *101*, 1267.
[50] O. Allemann, S. Duttwyler, P. Romanato, K. K. Baldridge, J. S. Siegel, *Science* **2011**, *332*, 574.
[51] C. Sánchez-Sánchez, S. Brüller, H. Sachdev, K. Müllen, M. Krieg, H. F. Bettinger, A. Nicolaï, V. Meunier, L. Talirz, R. Fasel, P. Ruffieux, *ACS Nano* **2015**, *9*, 9228.